



Comparison of corneal endothelial mosaic according to the age: the corimmo 3D project

Klervi Rannou, Emmanuel Crouzet, Caroline Ronin, Patricio Guerrero, Gilles Thuret, Philippe Gain, Jean-Charles Pinoli, Yann Gavet

► To cite this version:

Klervi Rannou, Emmanuel Crouzet, Caroline Ronin, Patricio Guerrero, Gilles Thuret, et al.. Comparison of corneal endothelial mosaic according to the age: the corimmo 3D project. IRBM, Elsevier Masson, 2016, 37 (2), pp.124-130. <<http://www.sciencedirect.com/science/article/pii/S1959031816300069>>. <10.1016/j.irbm.2016.03.004>. <hal-01365604>

HAL Id: hal-01365604

<https://hal.archives-ouvertes.fr/hal-01365604>

Submitted on 15 Sep 2016

HAL is a multi-disciplinary open access archive for the deposit and dissemination of scientific research documents, whether they are published or not. The documents may come from teaching and research institutions in France or abroad, or from public or private research centers.

L'archive ouverte pluridisciplinaire **HAL**, est destinée au dépôt et à la diffusion de documents scientifiques de niveau recherche, publiés ou non, émanant des établissements d'enseignement et de recherche français ou étrangers, des laboratoires publics ou privés.

Comparison of corneal endothelial mosaic according to the age : the CorImMo 3D project

K. Rannou^{a,*}, E. Crouzet^b, C. Ronin^b, P. Guerrero^a, G. Thuret^{b,c}, P. Gain^b, J.C. Pinoli^a, Y. Gavet^a

^a*École Nationale Supérieure des Mines de Saint-Étienne, LGF UMR CNRS 5307, 158 cours Fauriel, CS 62362, 42023 Saint-Étienne, France*

^b*Corneal Graft Biology-Engineering and Imaging Laboratory, EA2521-Federative Institute of Research in Sciences and Health Engineering-Faculty of Medicine-Jean Monnet University, Saint-Étienne, France*

^c*Institut Universitaire de France, Boulevard St Michel, Paris, France*

Abstract

Aim: The human corneal endothelium is a monolayer of flat hexagonal cells. It is a nearly regular hexagonal tessellation during the first years of life, but with age, becomes less regular in shape and size. The aim is to evaluate geometrically the age of an endothelial mosaic.

Material and methods: Segmented endothelial mosaics of healthy subjects of different age groups are compared by morphological criteria. The mosaics are studied according to their age group (decades), their age and their location (center or mid-periphery of the cornea). The measures used are : the cell density, the Ripley's L function and the cell area and perimeter density.

Results: These measures point out the endothelial cell density decrease, the cell area, perimeter and diameter increase, the cell heterogeneity increase, and the differences between central and mid-peripheral cells increases with

*Corresponding author

Email address: klervi.rannou@emse.fr (K. Rannou)

age.

Conclusion: These measures are able to characterize healthy mosaics.

Keywords: corneal endothelium, cell morphology, Ripley's function, area density, perimeter density

1. Introduction

The human corneal endothelium is a monolayer of flat hexagonal cells, which do not regenerate and are responsible for the maintenance of the cornea transparency. When the number of endothelial cells (ECs) is too low, the cornea becomes edematous, causing irreversible loss of vision that can only be treated by a corneal graft. The donor cornea brings numerous new functioning ECs into the recipient eye. Because of their location at the most posterior layer of this transparent tissue, ECs can be visualized in vivo using a specular microscope using the light reflected by the interface between ECs and the liquid that fills the anterior chamber of the eye. Similarly, they can be observed ex vivo during corneal storage using a transmitted light microscope or a specular microscope. The morphologic characteristics of ECs have been studied since the 50's. Three parameters are universally used to describe the endothelium: the EC density (ECD, by convention expressed in cells/mm²), the coefficient of variation of cell area indicative of the pleomorphism (CV is the standard deviation divided by the mean cell area), and percentage of cells with 6 neighbors, indicative of polymorphism (hexagonality).

During the first years of life, the endothelial mosaic is a nearly regular hexagonal tessellation. With aging, endothelial cells (ECs) become less regular in shape and size and their number slowly decreases, at a rate of 0.6% per

21 year during adulthood [1]. Nevertheless, in healthy corneas, the number of
22 ECs remains always high enough to maintain corneal clarity even in centenar-
23 ians. This important notion of endothelial reserve disappears when diseases
24 or traumatism alter the endothelium. In these situations, decrease of ECD
25 and changes in pleomorphism (i.e. shape variability) and polymorphism (i.e.
26 size variability) can be dramatically accelerated, ultimately leading to corneal
27 opacification requiring corneal graft.

28 In eye banks, donor corneas are stored and strictly controlled in order
29 to verify if they are suitable for corneal graft. Quality of the endothelium
30 is the main criterion to decide whether a cornea can be grafted or must be
31 destroyed. At present, ECD is the only quantitative parameter used. A
32 threshold under which a cornea is unsuitable for graft determines the fate
33 of each donor cornea. It is usually of 2000 cells/mm² for corneas destined
34 to penetrating keratoplasty (replacement of the whole thickness of the cen-
35 tral cornea, constituting the gold standard and the most frequent technique
36 worldwide) and 2400 cells/mm² for corneas destined to posterior endothelial
37 graft (selective replacement of the endothelium, requiring preparation of a
38 thin posterior lamellae that can be slightly harmful to the ECs, explaining
39 the higher threshold). For CV and hexagonality that can be measured with
40 image analysis [2], their influence on the post graft endothelial survival has
41 never been studied. They are at present used as additional criteria to help
42 qualifying corneas with ECD near the threshold.

43 In order to better explain endothelial aging and some of the most frequent
44 clinical situations (ECD decrease in Fuchs corneal endothelial dystrophy, the
45 most frequent primary endothelial dystrophy, and after corneal grafts), new

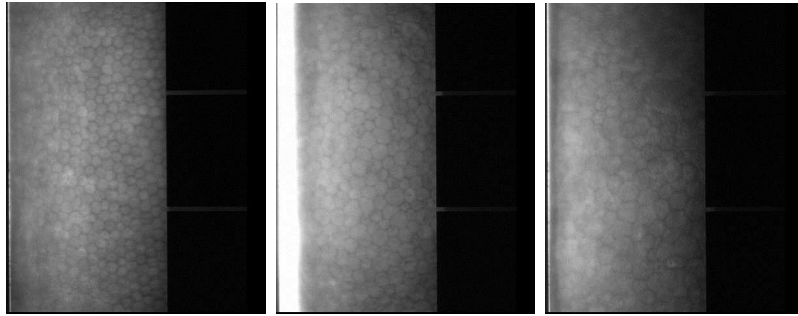
46 methods to qualify the endothelial mosaic, using geometrical and morpho-
47 logical criteria, are studied. The aim is to establish an original mathematical
48 model of the human corneal endothelium. In the present work, three mea-
49 sures of the cell size variability are presented: the Ripley's L function and
50 the area and perimeter cells densities. These mathematical parameters are
51 used to assess the age of an endothelial mosaic of healthy corneas.

52 **2. Material and methods**

53 *2.1. Source of endothelial images*

54 Images were taken using a small field non-contact specular microscope
55 (SP 3000, Topcon, Tokyo, Japan) (Fig.1). In 10 age groups (from 0 to 10
56 years old, 11 to 20, 21 to 30, . . . , and 91 to 100), images of healthy eyes of 5
57 subjects that were taken during routine examination, were selected. Images
58 were anonymised and patients could not be recognized from the pictures.

59 ECD is not homogeneous on the whole endothelium, it progressively de-
60 creases toward center ([4, 3]). For each eye, five images were therefore taken
61 in the central, temporal, nasal, superior and the inferior zones of the en-
62 dothelium, by asking the patient to focus on each of the 5 LEDs placed on
63 the microscope to orientate the eyeball. The 4 non central positions were
64 localized 3 to 4 millimeter from the center, that is to say not in the extreme
65 periphery of the cornea. As non-contact specular microcope have a narrow
66 field of view, the acquisition of 5 images distributed on the corneal surface
67 is the usual protocol used in routine to increase the sampling and obtain a
68 more representative analysis. Each image was manually segmented by an
69 expert using ImageJ (Fig.2).



(a) Central 4-year-old patient (b) Central 41-year-old patient (c) Central 92-year-old patient

Figure 1: Representative images of the endothelial mosaic taken using a small field non-contact specular microscope.

70 *2.2. Ripley's L function*

71 The Ripley's L function (RLF) is used to analyze the spatial distribution
 72 of a collection of points. The RLF counts the mean number of mass centers
 73 at a given distance from another mass center [5, 6].

74 Let $P = \{p_1, p_2, \dots, p_N\}$ be a collection of N points in the image I ,
 75 considered as a bounded region of \mathbb{R}^2 , and let A be the area of I .

76 An estimator of the RLF is given, for all $r \geq 0$, by:

$$\hat{L}(r) = \sqrt{\frac{A}{\pi N^2} \sum_{i=1}^N \sum_{j \neq i} \delta_{ij}(r)}, \quad (1)$$

77 where $\delta_{ij}(r)$ is equal to 1 if the distance between the points p_i and p_j is less
 78 than r , and 0 otherwise.

79 The RLF is compared to the stationary Poisson point process one, that
 80 serves as a measure of complete randomness and lack of interaction. In the
 81 case of a Poisson point process, $L(r) = r$ for all distance r . Moreover, for

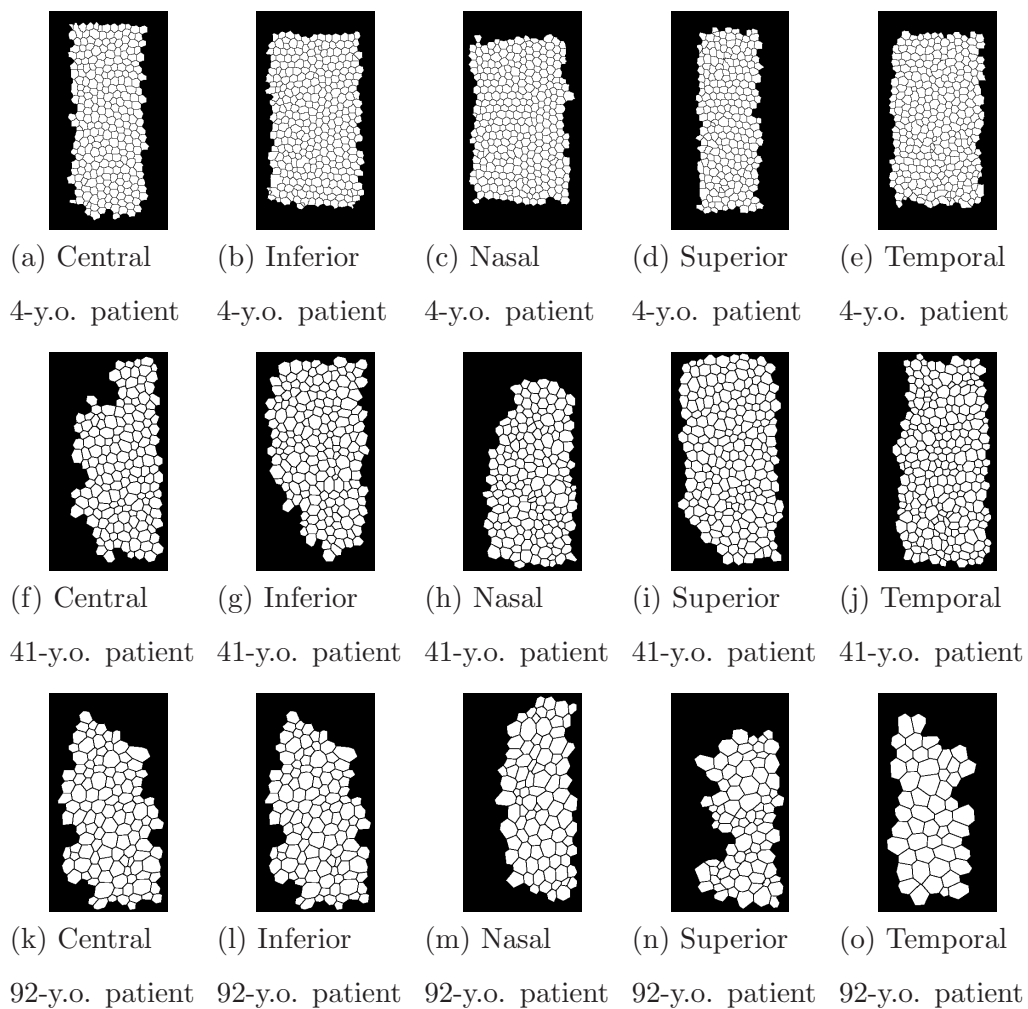
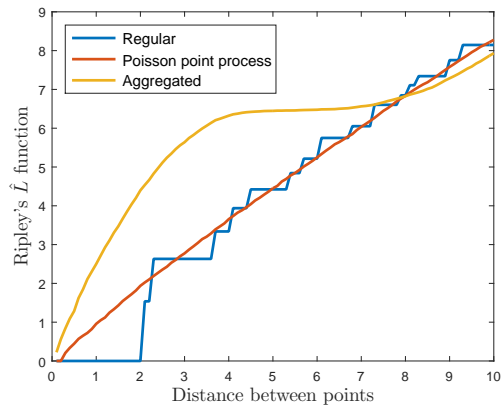
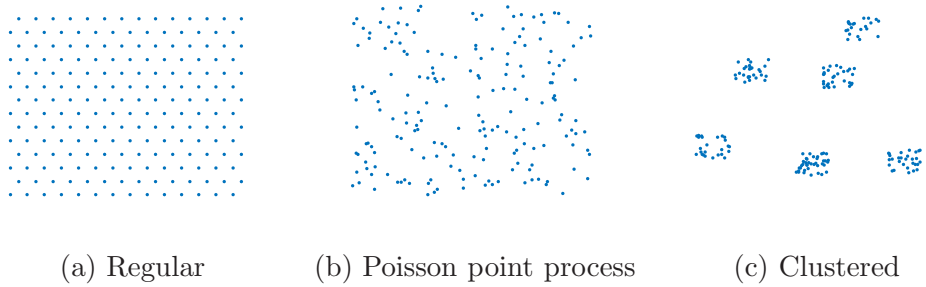


Figure 2: Representative segmented endothelial mosaics of the central, inferior, nasal, superior and temporal zones of the right eye of three patients. They illustrate that cell area, the polymorphism and pleomorphism increase with age.



(d) Ripley's \hat{L} function

Figure 3: Three collections of points and their Ripley's \hat{L} function. (a) is a regular point collection, \hat{L} is a step function and for small distances, $\hat{L}(r) < r$. (b) is a realization of a Poisson point process, \hat{L} is linear. (c) are clustered points, $\hat{L}(r) > r$.

82 small distances, $L(r) < r$ indicates regularity and $L(r) > r$ aggregation
 83 (Fig.3).

84 In the case of the endothelial mosaic, the points considered are the mass
 85 centers of the ECs. The RLF provides information about the spatial distribu-
 86 tion of the cells mass centers, and consequently about the distance between
 87 cells mass centers, that is to say their diameters.

88 *2.3. Area and perimeter density*

89 Another way to study the cell size variability according to the age, is to
90 use the area and perimeter density of ECs.

91 Let (a_1, \dots, a_k) be a sample of observations : cell area or perimeter (of
92 a patient, or an age group, etc.). The density function f of this sample is
93 estimated by the kernel density estimator [7, 8], which is:

$$\hat{f}(x) := \frac{1}{bk} \sum_{i=1}^k K\left(\frac{x - a_i}{b}\right), \quad (2)$$

94 where $K(\cdot)$ is a kernel function and $b > 0$ is the smoothness parameter, called
95 bandwidth, proportional to $k^{-\frac{1}{5}}$. The kernel function used is the Epanech-
96 nikov kernel function [9].

97 A kernel density estimator is used rather than an histogram, because the
98 histogram method have fixed classes whereas the kernel estimator is mobile
99 and centered on each observation.

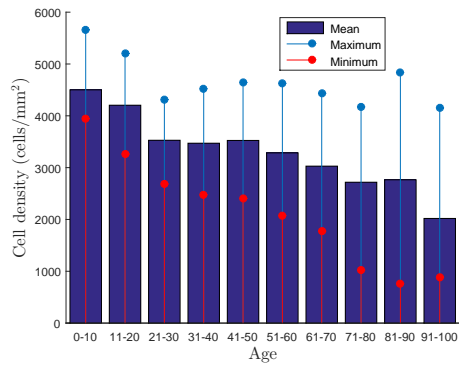
100 **3. Results**

101 *3.1. Endothelial cell density*

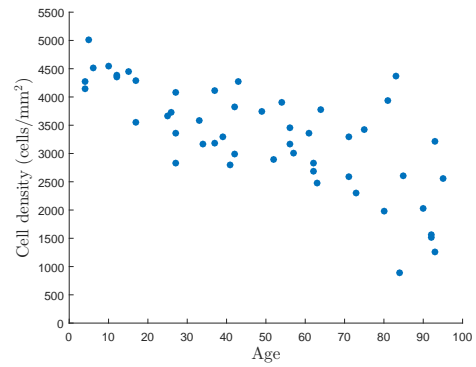
102 First, the mean ECD per age group and per patient is calculated over
103 all images of an age group or patient (Fig.4a and 4b). As expected, ECD
104 decreased with age and the variability between patients of the same age class
105 increased (the coefficient of variation computed over all images of an age
106 group increases, Fig.4c).

107 *3.2. Ripley's L function*

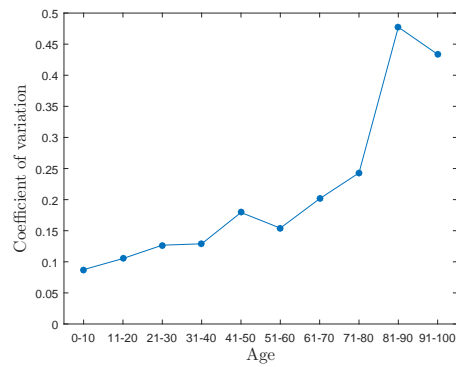
108 The \hat{L} function was calculated for the cell mass centers of each segmented
109 image of an age group. The mean \hat{L} function over all images of an age group



(a) ECD per age group



(b) ECD per patient



(c) Coefficient of variation per age group

Figure 4: (a) Mean, minimum and maximal endothelial cell density of all images of each age group, (b) mean cell density for each patient, and (c) the coefficient of variation for each age group.

110 was then represented graphically, and compared to the one of realizations of
 111 Poisson point processes (Fig.5a). For all age groups, the mean \hat{L} function is
 112 null for small distances and become non null earlier for the youngest group,
 113 meaning that the smallest distance between mass centers increases with age.
 114 Oscillations of the mean RLF were marked for the youngest age groups and
 115 decreased with age, indicating that homogeneity in cell diameters decreased
 116 with age. Furthermore, the first rebound for the youngest age groups indi-
 117 cates the maximum distance between mass centers of neighbor cells.

118 For 3 age groups (young: 0-10 years old, middle age: 41-50 years old, and
 119 elderly age: 91-100 years old), we compared the RLF of the ECs from the
 120 center of the cornea with the mean RLF of the 4 images taken in the mid
 121 periphery of the cornea (Fig.5b).

122 To quantify the difference between two curves, the error in percent was
 123 compute between the curve of the central \mathcal{C}_1 and the mid peripheral cells \mathcal{C}_2 :

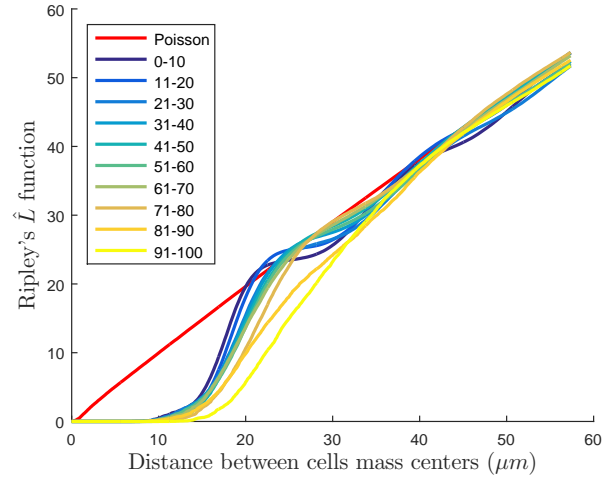
$$E(\mathcal{C}_1, \mathcal{C}_2) = \frac{\|\mathcal{C}_1 - \mathcal{C}_2\|_1}{\frac{1}{2}\|\mathcal{C}_1 + \mathcal{C}_2\|_1} \times 100, \quad (3)$$

124 where $\|\cdot\|_1$ is the l_1 norm (also called Manhattan or Taxicab norm). No big
 125 difference was observed between center and mid periphery ($E < 1\%$), except
 126 for the elderly age group (Fig.6), but it is probably due to the small number
 127 of cells per image for some elderly patients.

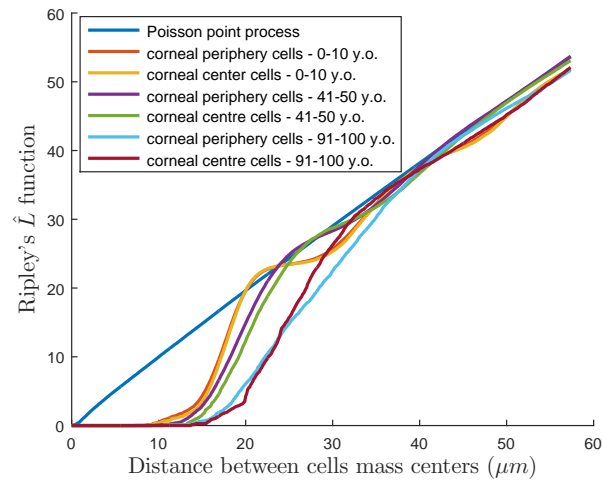
128 3.3. Area and perimeter density

129

130 The standard deviation of the cell area and perimeter mean estimate
 131 density progressively increases with age (wider dispersion around the peak),
 132 and indicates a gradual increase in heterogeneity (Fig.7). The function E (3)



(a)



(b)

Figure 5: The mean Ripley's \hat{L} function for realizations of a Poisson point process and for endothelial mosaics. The mean \hat{L} function (a) for each age group and (b) for cells observed in the center versus in the mid periphery of the cornea in 3 age groups.

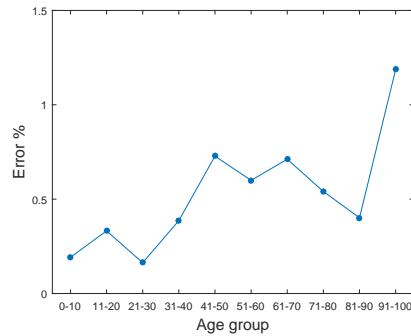
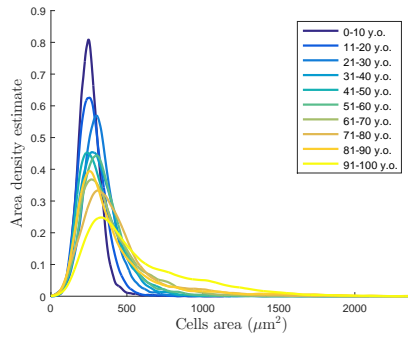


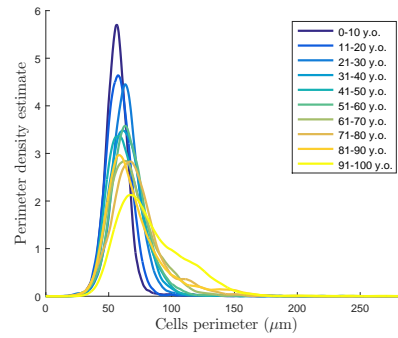
Figure 6: Error between the mean Ripley's \hat{L} function of center and mid peripheral endothelial cells.

133 was calculated for each patient between his density mean estimate and his
 134 age group density mean estimate, to quantify the inter-individual variability
 135 in each age group, and showed the increase of inter-individual variability
 136 (Fig.8a).

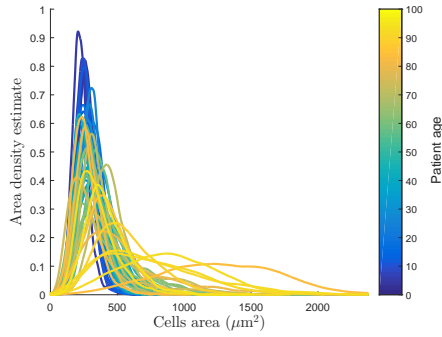
137 Next, the cell area and perimeter estimate density of the central cells was
 138 compared to the mean estimates densities of the mid peripheral cells for 3
 139 age groups (Fig.7e-7f). For the two oldest age groups, the mean cell area
 140 and perimeter (density peak) is higher in the central cells than in the mid
 141 periphery of the cornea, indicating that, with age, the central cells become
 142 bigger than in the mid periphery. The computation of the E function, be-
 143 tween densities mean estimates of central and mid peripheral ECs, pointed
 144 out these increases of differences between center and mean periphery with
 145 age (Fig.8b).



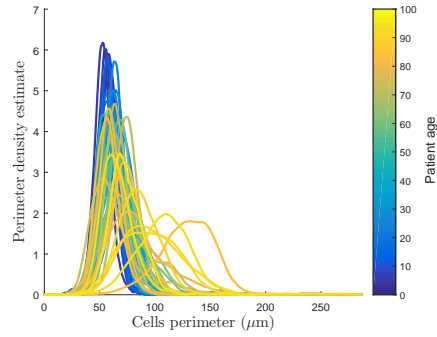
(a) Area



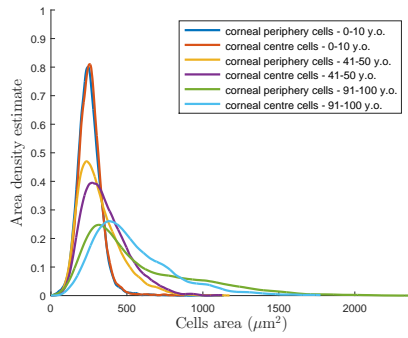
(b) Perimeter



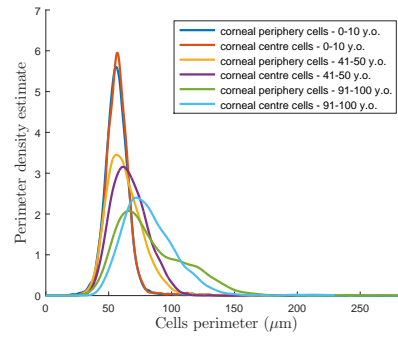
(c) Area



(d) Perimeter



(e) Area



(f) Perimeter

Figure 7: Cells area and perimeter density **mean** estimate. (a)-(b) for each age group, (c)-(d) for each patient, and (e)-(f) for cells observed in the center versus in the mid periphery of the cornea in 3 age groups.

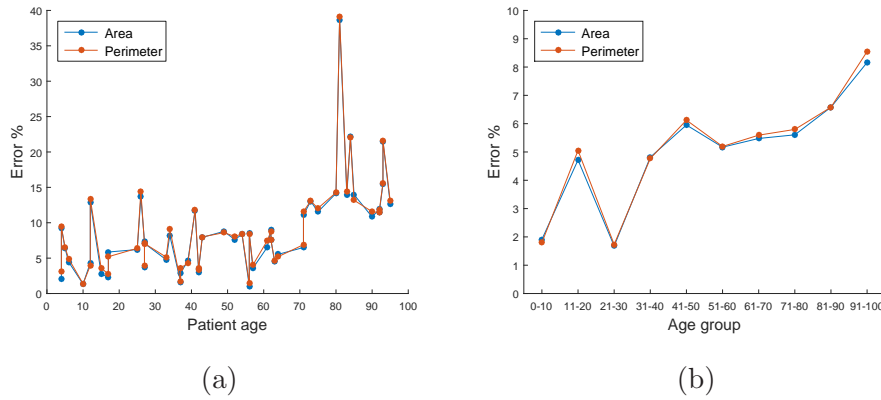


Figure 8: Error between area and perimeter densities mean estimates : (a) between the mean age group curve and each patient curve, to quantify the variability between patients, and (b) for each age group, between the curves of the center and the mid peripheral endothelial cells.

146 4. Discussion

147 The number of subjects is quiet low per decade, and for the oldest groups,
 148 the small field of observation of the non-contact microscope was an obstacle
 149 because it greatly limited the number of entirely visible big ECs. Therefore,
 150 a great number of ECs were available to analyze the endothelial mosaic per
 151 decade, but not to study them image per image or to compare central cells to
 152 outlying cells for some subjects. Repeating the analysis with more subjects
 153 and using wide field digital contact specular microscopy images [10] would
 154 validate and improve the accuracy of our measurements. Further works are
 155 ongoing to constitute a bank of images of wide field digital contact specular
 156 microscopy images.

157 Despite the time-consuming task, the segmentation have been made man-
 158 ually by an expert to avoid the bias induced by automatic segmentation

159 methods, and in order that the segmented endothelial mosaics serve as ref-
160 erence.

161 In this preliminary study, it has been shown that the ECD, the RLF and
162 the area and perimeter density estimate are able to characterize the human
163 corneal endothelial mosaic changes occurring with age. These measures point
164 out the differences according to the age : they find the same well-known in-
165 crease in cell area (diameter and perimeter) and increase in cell heterogeneity,
166 they point out that inter-individual variability increases and that a difference
167 between size of ECs from the central (bigger) and the mid-peripheral cornea
168 appears with age. The time needed to compute all these measures is quite
169 low : the mean time for one view is 0.63 seconds (the maximum time is 1.32
170 seconds).

171 **5. Conclusion**

172 Original geometrical and morphological criteria are able to characterize
173 the healthy human corneal endothelial mosaic. Works are now ongoing to
174 study other parameters like the number of neighbor cells, morphometric cri-
175 teria by using shape diagrams [11], etc. Applied to the most frequent patho-
176 logical endothelial modifications (ECs loss after corneal grafts and in Fuchs
177 corneal endothelial dystrophy), these new criteria could bring new insights
178 in their physiopathology.

179 **Acknowledgments**

180 The authors wish to thank the French National Research Agency for
181 financial support (ANR-12-TECS-004, CorImMo 3D).

182 **References**

- 183 [1] W. M. Bourne, L. R. Nelson, D. O. Hodge, Central corneal endothelial
184 cell changes over a ten-year period., *Invest Ophth Vis Sci* 38 (3) (1997)
185 779–82.
- 186 [2] S. Acquart, P. Gain, M. Zhao, Y. Gavet, A. Defreyne, S. Piselli, et al.,
187 Endothelial morphometry by image analysis of corneas organ cultured
188 at 31 degrees c., *Invest Ophth Vis Sci* 51 (3) (2010) 1356–64.
- 189 [3] B., Schimmelpfennig, Direct and indirect determination of nonuniform
190 cell density distribution in human corneal endothelium, *Invest Ophth*
191 *Vis Sci* 25 (2) (1984) 223–9.
- 192 [4] Z. He, N. Campolmi, P. Gain, B. M. Ha Thi, J.-M. Dumollard,
193 S. Duband, et al., Revisited microanatomy of the corneal endothelial pe-
194 riphery: new evidence for continuous centripetal migration of endothelial
195 cells in humans, *Stem Cells* 30 (11) (2012) 2523–34.
- 196 [5] B. D. Ripley, Modelling spatial patterns, *J. R. Stat. Soc. Ser. B Stat.*
197 *Methodol.* (1977) 172–212.
- 198 [6] M. N. M. vanLieshout, A. J. Baddeley, A nonparametric measure of
199 spatial interaction in point patterns, *Stat. Neerl.* 50 (3) (1996) 344–61.
- 200 [7] M. Rosenblatt, Remarks on some nonparametric estimates of a density
201 function, *Ann. Math. Stat.* 27 (3) (1956) 832–7.
- 202 [8] E. Parzen, On estimation of a probability density function and mode,
203 *Ann. Math. Stat.* (1962) 1065–76.

- 204 [9] V. A. Epanechnikov, Non-parametric estimation of a multivariate prob-
205 ability density, *Theor Probab Appl+* 14 (1) (1969) 153–8.
- 206 [10] G. Hor, Y. Gavet, A. Bernard, C. Urrea, P. Gain, G. Thuret, Digi-
207 talization of a wide field contact specular microscope leads to better
208 performances, 2016. Manuscript submitted for publication.
- 209 [11] K. Rannou, Y. Gavet, J.-C. Pinoli, Characterization of the corneal en-
210 dothelial mosaic and comparison with simulated tessellations modeled
211 with gaussian random fields, in: *The International Conference on Qual-
212 ity Control by Artificial Vision 2015*, International Society for Optics
213 and Photonics, 2015.